FINAL TECHNICAL REPORT

Participation in the Mars Orbiting Laser Altimeter Experiment

NASA Grant NAG5-4434

Principal Investigator: Professor Gordon H. Pettengill
Rm 37-582d, Mass. Inst. of Technology
Cambridge, Mass. 02139-4307
Tel: (617) 253-4281

Award Period: 12/31/97 to 12/31/02

Total Amount Awarded: $409,282.00

1. GRANT MISSION

This NASA Grant, 5-4434, has covered the active participation of the Principal Investigator, Prof. Gordon Pettengill, and his Co-Investigator, Peter Ford, in the Mars Orbiting Laser Altimeter (MOLA) Experiment, over a period of five years. This participation has included attending team meetings, planning observing operations, developing data-reduction software algorithms, and processing data, as well as presenting a number of oral reports at scientific meetings and published papers in refereed journals. This research has concentrated on the various types of Martian clouds that were detected by the laser altimeter, with results summarized below and published in the journal articles listed in Section 4.

2. TECHNICAL SUMMARY

The Mars Orbiting Laser Altimeter (MOLA) instrument [1,2] carried aboard the Mars Global Surveyor (MGS) spacecraft, has observed strong echoes from cloud tops at 1.064 μm on 61% of its orbital passes over the winter north pole ($235° < L_s < 315°$) and on 58% of the passes over the winter south pole ($45° < L_s < 135°$). The clouds are unlikely to be composed of water ice since the vapor pressure of H_2O is very low at the Martian nighttime polar temperatures measured by the Thermal Emission Spectrometer (TES) [3], and by an analysis of MGS radio occultations [4]. Dust clouds can also be ruled out since no correlation is seen between clouds and global dust storms. The virtually certain composition for the winter polar clouds is CO_2 ice.

We have constructed a database of MOLA clouds, identified by clusters of closely grouped echoes lying significantly above the planetary surface. Each set of cloud echoes was plotted by altitude and along-track distance (see Figs. 3–5), inspected visually, and assigned to a category based on its morphology and relation to surface features. The location of clouds by latitude, sub-solar longitude (L_s), and solar incidence angle are shown in Figs. 1 and 2.

The colors used to denote the cloud locations in Figs. 1 and 2 indicate the categories that we have assigned to them, as exemplified in Figs. 3–5 which show the altitude (km) and distance-along-track (km) of typical lidar echoes for the three most common categories.

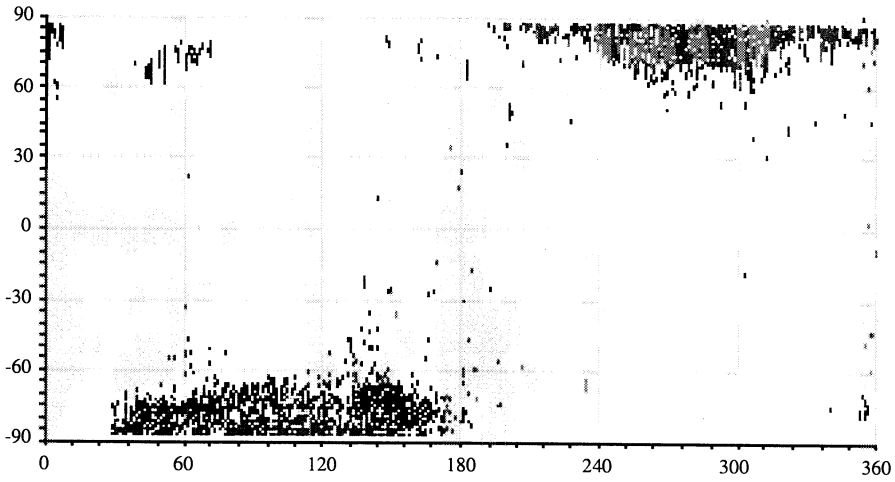

Fig. 1: Location of MOLA clouds by latitude (ordinate) and sub-solar longitude, L_S (abscissa).

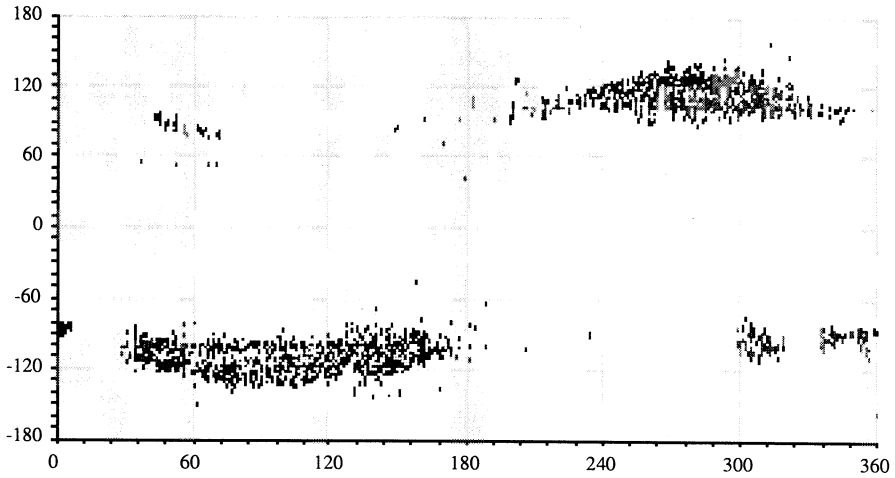

Fig. 2: Location of MOLA clouds by solar incidence angle (ordinate)and sub-solar longitude, L_S.(abscissa). Values of solar incidence greater than +90° or less than –90° indicate that the sun is below the horizon.

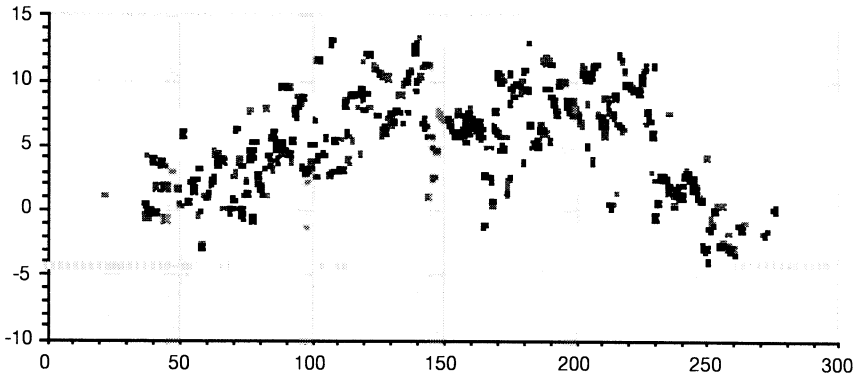

Fig. 3: Echoes from a typical cloud formation that is adjudged to contain *propagating* waves—green in Figs. 1 and 2—which are more common in the northern than in the southern polar regions. Ordinate represents altitude (km) and abscissa distance along track (km).

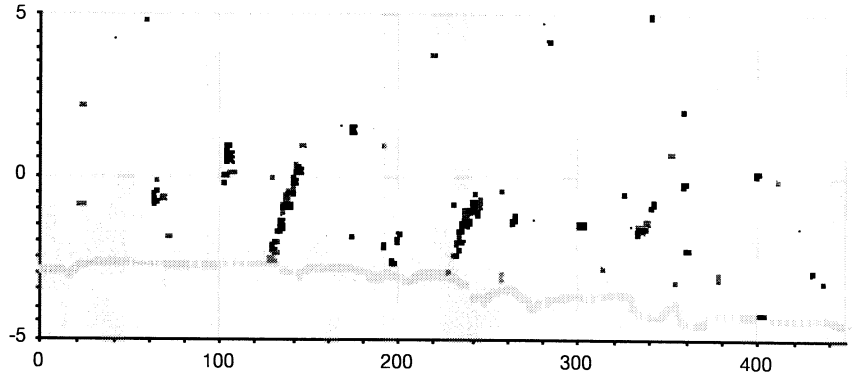

Fig. 4: Example of clouds associated with *topographic* features—colored blue in Figs. 1 and 2—with the appearance of mountain waves or perhaps snow tails. Ordinate represents altitude (km) and abscissa distance along track (km).

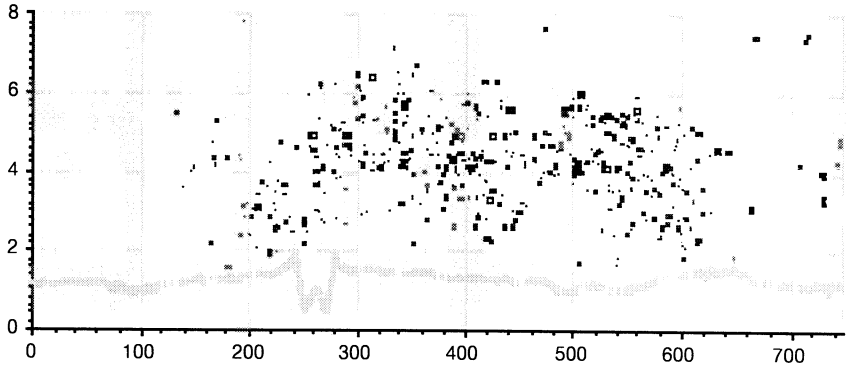

Fig. 5: Example of *diffuse* clouds—colored red in Figs. 1 and 2—whose lidar echoes show very little time dispersion. They are seen only in southern polar latitudes. Ordinate represents altitude (km) and abscissa distance along track (km).

Less common categories are *dome-shaped* clouds (colored light blue in Figs. 1 and 2), dense isolated formations not apparently associated with surface features, *ground-hugging* clouds (magenta), flat clouds that form at altitudes of less than 1 km in the spring and autumn dawn, and occasional *crater clouds* (brown), which form within large impact craters.

The data points in Figs. 3–5 have been color coded according to the time dispersion of the lidar echoes: red indicates reflection from a cloud top whose density onset varies strongly over no more than 3m of range; green and yellow denote intermediate gradients; while the blue echoes are the most dispersed in range—from clouds whose density discontinuity is spread over 90m or more. Cloud echoes that saturated the MOLA receiver are colored magenta, and surface echoes are colored grey.

Under conditions of Mie scattering, and assuming unit geometric albedo, the number density of CO_2 ice particles required to produce the observed echo strengths is about $2 \times 10^8 r^{-2}$ per m^3, where r is the particle radius in μm, which we infer to lie between 0.1μm and 50 μm. If r were less than 0.1μm, Rayleigh scattering would predominate, the cross-section would rapidly drop off as r^{-4}, and no lidar echo would be detectable. If r were greater than 50μm, the particles would fall too fast to sustain the observed wavefront patterns.

In addition to these reflective clouds, MOLA often receives no echo from either cloud or surface, thus implying an intervening absorbing medium. These *non-reflective* or absorbing clouds form a distinct category. Since they are not exclusive to the polar night, and are more common during hemispheric dust storms, they may be composed largely of dust or diffuse H_2O ice, rather than CO_2 ice.

Buoyancy Waves. We have identified and measured all lineaments within the cloud-top echoes, such as those visible in Figs. 3 and 4. We assume that the multiple wave fronts of the *propagating* class (Fig. 3) are buoyancy waves moving through a CO_2 atmosphere [5]. Particles of dry ice are alternately condensed and evaporated as the ambient temperature is modulated above and below the local freezing point by the passing wave. This implies that the atmosphere is close to its "wet" CO_2 adiabat at ~148K, at which point the buoyancy frequency is estimated to be $\sim 9.31 \times 10^{-3}$ rad/s.

Spatial-Temporal Correlation. The combination of the MGS sun-synchronous orbital period, ~7061 s, and the length of the Martian day, ~88775 s, results in a near overlap of surface tracks at 7-day (88 orbit) intervals. However, since the tracks culminate (converge) at ±86° latitude, more frequent overlaps occur at polar latitudes. We therefore auto-correlated the locations of all clouds of a given category, assuming that they circle with the ambient wind around the pole, at a nominal zonal flow. Fig. 6 shows the result of these correlations around the south pole, for a range of assumed zonal rotation rates.

Note the strong correlation at non-zero rotation rate for the class of *propagating* clouds (*e.g.*, Fig. 3) and the relatively weak correlation between clouds related to *topographic* features (*e.g.*, Fig. 4), suggesting that the former are moving in a polar vortex—*ca.* 5 m/s at 75°S latitude—while the latter are not. The tracks of some correlated propagating clouds are shown in Fig. 7.

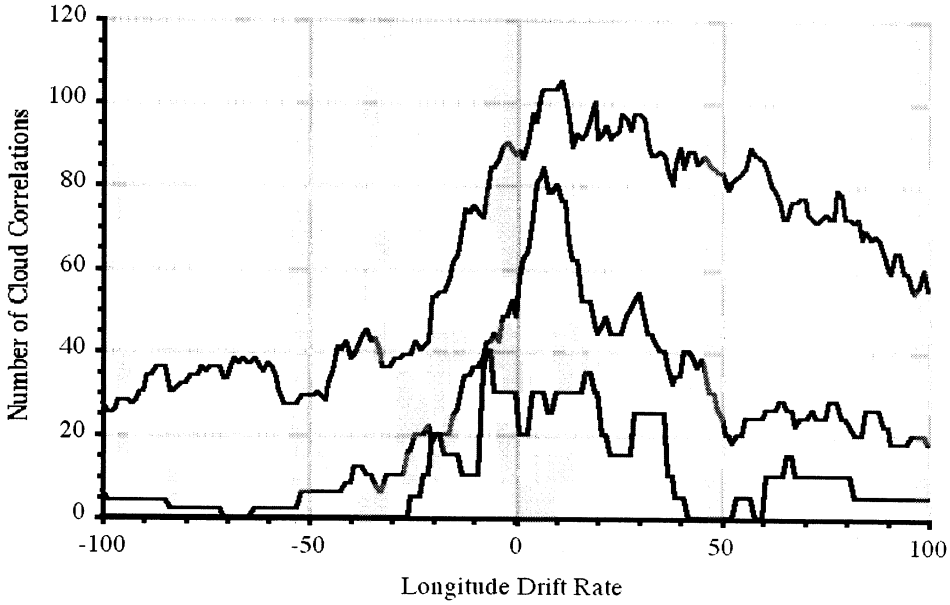

Fig. 6 Correlation between pairs of clouds detected within 48 hours of each other and separated by > 1° of arc measured from the center of Mars, as a function of zonal vortex wind drift rate (degrees of longitude per day). Green: correlation of propagating clouds; blue: of topographic clouds; black: of all cloud categories.

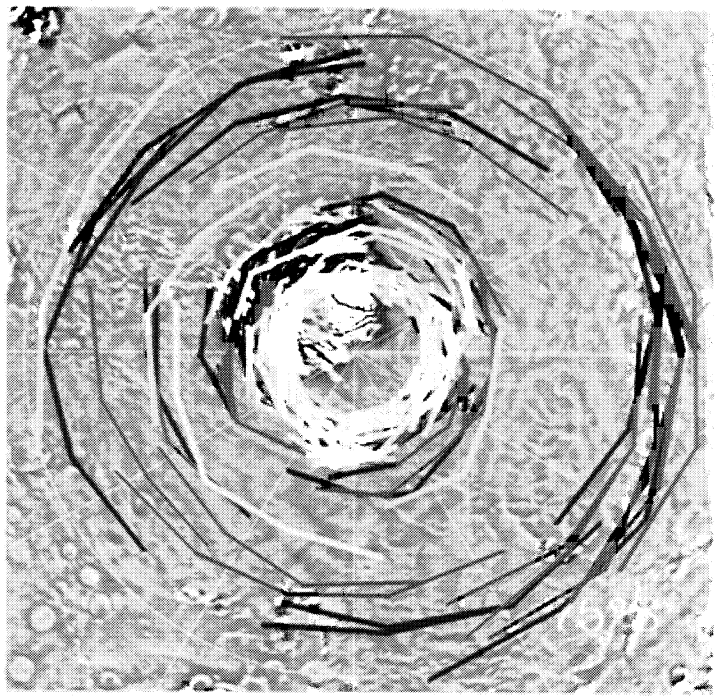

Fig. 7: Track history of correlated clouds near the South Pole of Mars. Color denotes the interval over which correlation was observed: pink: 1 day; green: 2 days; blue: 3 days; cyan: 4 days.

Infrared Emission. Simultaneous observations were made by MOLA and by the MGS Thermal Emission Spectrometer (TES) [6]. At the low temperatures of the polar night, the emission spectrum E(λ) between 15μm and 25μm is most useful. With minimal contribution from H_2O and dust, the emission is dominated by the CO_2 rotation band at 15μm and by the thermal (Planck) spectrum from the surface and atmosphere at their respective temperatures. Although the fundamental spatial resolution of each of the 6 TES detectors is ~3×3 km, all six are usually summed together for polar nighttime observations in order to achieve detectable signal levels. Each footprint is therefore ~6×9 km and encloses the ~200 m diameter MOLA footprint. The surface emissivity is typically ~0.95 at these wavelengths, so most TES observations in the polar night (see Fig. 8) show an atmosphere and surface at ~148K.

Anomalous "cold spots" have been observed in the polar night, however, both by TES and by the IRIS instrument on Mariner 9 [7]. Fig. 8 shows TES spectra at three latitudes. On the left, at 60°S, the warm sunlit atmosphere emits strongly at 15μm, but is almost transparent at other wavelengths, which are dominated by surface emission. At 85.5°S, the atmosphere is colder than the surface and absorbs at 15 μm, while the radiometric temperature drops at $\lambda > 20\mu m$, indicating an anomalous "cold spot." At 79.5°S, the long-wavelength anomaly disappears and only the 15μm absorption feature remains.

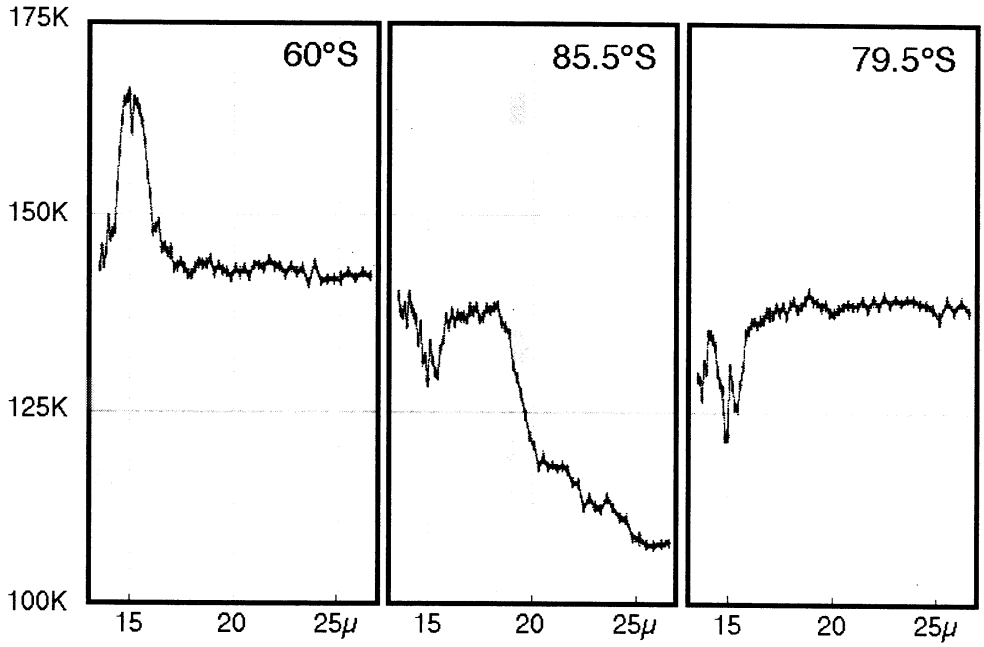

Fig. 8: Infrared TES emission spectra at three latitudes in the same pass (orbit 18799, L_S = 122°).

Three explanations for the cold spots have been put forward. They could result from CO_2 ice clouds [8], from a deep layer of CO_2 frost [8,9], or from surface layers of CO_2 slab ice [10]. In each case, the low value of emissivity results from volume scattering, but under very different conditions. To choose among these models, we have made maps of the spectral slope, $\partial E/\partial\lambda$, for $20\mu m < \lambda < 25\mu m$ at intervals of 5° in L_s. The cold spots show up clearly as isolated minima, as shown in Fig. 9.

Having identified a particular cold spot, we note the first time at which TES detected it and the last previous time, if any, at which TES observed that region without detecting an anomaly. From these data, an estimate of the average lifetime of a cold spot can be determined. We have also correlated MOLA clouds against TES cold spots, to test whether the two are related, and whether particular types of cloud may be responsible. At the present time, it appears as though there is little correlation, but attempts continue.

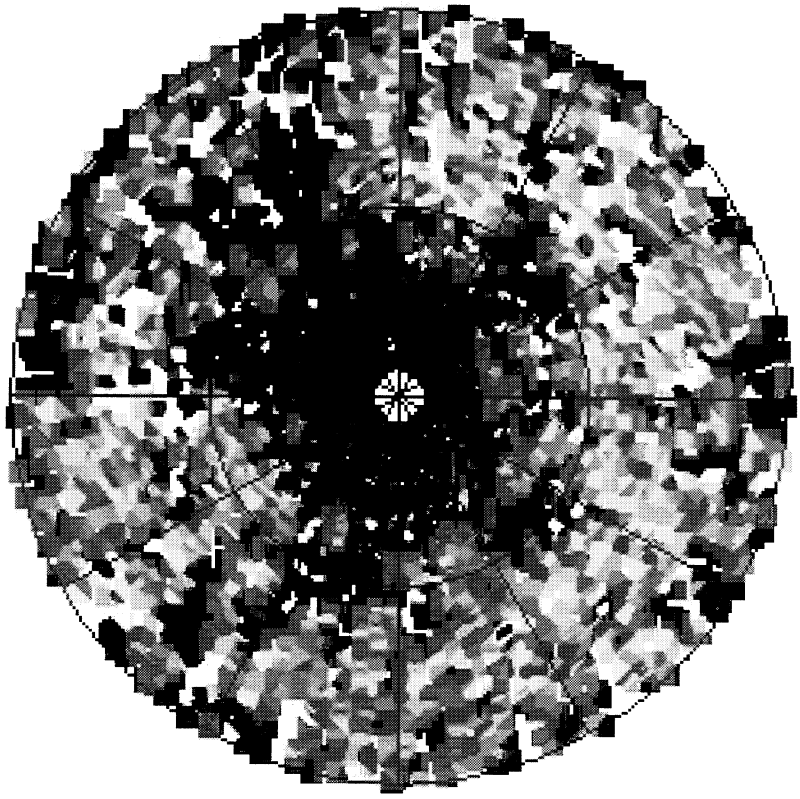

Fig. 9: Map of the TES spectral slope, $\partial E/\partial\lambda$, for $20\mu m < \lambda < 25\mu m$, $70° < L_S < 80°$ in the southern winter. Cold spots (blue, magenta) are clearly visible with negative spectral slopes.

References

[1] Zuber *et al.*, J. Geophys. Res., **97**, 7781 (1992)

[2] Zuber *et al.*, Science, **282**, 2053 (1998)

[3] Christensen *et al.*, J. Geophys. Res., **106**, 23823 (2001)

[4] Hinson *et al.*, J. Geophys. Res., **106**, 1463 (2001)

[5] Pettengill and Ford, Geophys. Res. Lett., **27**, 609 (2000)

[6] Pearl *et al.*, J. Geophys. Res., **106**, 12325 (2001)

[7] Hanel *et al.*, Icarus, **17**, 423 (1972)

[8] Forget *et al.*, J. Geophys. Res., **100**, 21219, (1995)

[9] Ditteon and Kieffer, J. Geophys. Res., **84**, 8294 (1979)

[10] Titus et al., EOS Trans., **80**, 611 (1999

3. MEETINGS and PUBLICATIONS

Team Meetings: 20 meetings of the Laser Altimeter Team have been held during the reporting period; of these, the PI and/or the co-I have attended 19.

Professional Societies.

Am. Geophys. Un., San Francisco, December 1998; Peter Ford: *"Atmospheric Gravity Waves in the Martian North Polar Cap Winter;"* and Gordon Pettengill*: "Evidence for Cloud Condensation from a 'Wet' CO_2 Adiabat in the Martian Polar Winter."*

Am. Geophys. Un., San Francisco, December 1999,*"A Comparison of CO_2 Clouds over Both Martian Winter Poles, as Seen by MOLA;*

Eur. Geophys. Soc., Nice, April 2000; Peter Ford: *"Martian Polar Winter Cloud Wave-forms;"* and Gordon Pettengill: *"Structure of the Martian Polar Winter Atmosphere from Laser Observations."*

Mars Global Surveyor Water and Atmosphere Workshop, Boulder, June 2000, *"Martian Polar Clouds as Derived from MOLA Observations."*

Div. Plan. Sci. of the Am. Astron. Soc., Pasadena, October, 2000, *"The Motion of CO_2 Clouds over the Martian Winter Poles."*

Exploring Mars with TES: A Data User's Workshop, ASU, Tempe, November, 2001, *"Detecting Polar Clouds with TES and MOLA."*

Div. Plan. Sci. of the Am. Astron. Soc., New Orleans, November, 2001. *"The Infrared Signature of Martian Polar Clouds."*

Publications.

"Topography of the Northern Hemisphere of Mars from the Mars Orbiter Laser Altimeter," *Science*, **279**, 1686-1692 (1998); with 11 other authors from the MOLA Team.

"Observations of the North Polar Region of Mars from the Mars Orbiter Laser Altimeter," *Science*, **282**, 2053-2060 (1998); with 20 other authors from the MOLA Team.

"The Global Topography of Mars and Implications for Surface Evolution," *Science*, **284**, 1495-1503 (1999); with 18 other authors from the MOLA Team.

"Winter Clouds over the North Martian Polar Cap," *Geophys. Res. Ltrs* **27**, 609-612 (2000); G. H. Pettengill and P. G. Ford.

4. INVENTIONS

No patentable inventions have resulted from the research supported under this grant.